

Robust Direction-of-Arrival Estimation using Array Feedback Beamforming in Low SNR Scenarios

Parth Mehta[†], Kumar Appaiah *Member, IEEE*, and Rajbabu Velmurugan *Member, IEEE*

Abstract—A new spatial IIR beamformer based direction-of-arrival (DoA) estimation method is proposed in this paper. We propose a retransmission based spatial feedback method for an array of transmit and receive antennas that improves the performance parameters of a beamformer viz. half-power beamwidth (HPBW), side-lobe suppression, and directivity. Through quantitative comparison we show that our approach outperforms the previous feedback beamforming approach with a single transmit antenna, and the conventional beamformer. We then incorporate a retransmission based minimum variance distortionless response (MVDR) beamformer with the feedback beamforming setup. We propose two approaches, show that one approach is superior in terms of lower estimation error, and use that as the DoA estimation method. We then compare this approach with Multiple Signal Classification (MUSIC), Estimation of Parameters using Rotation Invariant Technique (ESPRIT), robust MVDR, nested-array MVDR, and reduced-dimension MVDR methods. The results show that at SNR levels of -60 dB to -10 dB, the angle estimation error of the proposed method is 20° less compared to that of prior methods.

Index Terms—Spatial IIR, Feedback, Array, Beamforming, Direction-of-Arrival (DoA)

I. INTRODUCTION

Beamforming is a well-studied concept in the field of spatial signal processing using antenna arrays. Spatial beamforming, along with direction estimation of the incoming signals and interference mitigation has received significant attention lately, especially for cognitive radar [1] systems, and systems wherein radar and communication need to coexist [2, 3]. Such coexistence necessitates robust beamforming with strong interference suppression, and accurate direction-of-arrival (DoA) estimation capabilities. The MVDR [4] beamformer is one candidate that offers simultaneous beamforming and interference suppression. Apart from beamforming, DoA estimation becomes an inherent part of the overall architecture. Typically, the signal that is received using spatial sensors is considered a sum-of-complex-exponentials along with additive white Gaussian noise. This particular model appears in a variety of applications, such as finite rate of innovation (FRI) sampling and denoising [5], target identification and classification [6, 7], and estimation of graph-dynamics [8]. With this model, the problem reduces to estimating the “frequency” parameter from the observed vector signal, as we discuss in Section II. Depending on the context of the problem, the notion of the “frequency” parameter changes. Extensive prior work has been done to estimate this frequency, using the MVDR method and other approaches. This includes subspace based

methods for DoA estimation such as MUSIC [9], ESPRIT [10] and their variants [11–15], filter based methods [16–18], and machine learning based methods [19, 20]. Several variants of the conventional MVDR [4] exist to enhance performance. One such method is robust MVDR [21, 22], that introduces an extra regularising parameter in the MVDR weight optimisation, that makes MVDR robust against the element-misalignments. Nested-array MVDR [23] is an interesting method that combines the concept of coarray with MVDR to enhance the degrees-of-freedom of the conventional method. Recently, MVDR using reduced dimension with subarrays [24] has been proposed, that divides the whole array into multiple subarrays, and performs MVDR for each of them in a serial fashion. One common aspect among all these prior works is that the estimation is based on a finite impulse response (FIR) model.

It is well-known that infinite impulse response (IIR) filters provide some advantages over FIR filters for several applications. Unlike FIR filters, an IIR filter’s transfer function has a numerator that accounts for the zeros of the transfer function and a denominator that accounts for poles of the transfer function. Due to the combined effect of both poles and zeros, IIR filters address some key issues with FIR filters [25] such as:

- Potentially offering a lower filter order for comparable performance.
- Offering a sharper roll-off for passband-stopband transitions.

While IIR filters offer these advantages, there are also some trade-offs that are involved when using IIR filters. These include a non-linear phase response, more complexity in optimizing coefficients etc. To this end, we ensure that the designs presented here are not affected by these shortcomings [26].

Prior work related to IIR filter based beamforming include [16, 18, 27, 28]. Most prior works consider direct implementation of the IIR filter by replacing the delay-and-sum FIR structure. Restructuring the delay-and-sum to individual IIR filters is explained in [16, 18] wherein it is proposed to replace the delays of the delay-and-sum with tap-delay IIR filters, and the filter coefficients are designed using the least-mean-square method iteratively. Extending this work in [27], the “spatial” delay elements are estimated using the recursive-least-squares method, which then can be used to estimate the spatial frequencies present in the signal. These architectures are largely an approximation, and use time-domain IIR filtering to achieve required desired spatial frequency response. To get an analogous spatial IIR structure,

the concept of ‘‘spatial feedback’’ has to be implemented, as discussed in [28]. Here, the authors propose to achieve this feedback by continuously retransmitting the beamformed signal to achieve IIR like performance.

In our work, we (a) consider that the retransmission is performed using an array instead of a single element, and (b) propose a method to incorporate the MVDR beamforming with this feedback structure to further improve the performance. This is an effective way to exploit the larger number of antennas available on MIMO wireless communication systems for more efficient DoA estimation. We first develop an optimal retransmission strategy that effectively utilizes the multitude of antennas by maximizing the Fisher information for the radar transceiver, and use this to infer the DoA. Through simulations, we first compare the performance parameters of the proposed method with conventional FIR beamformer and the single-element feedback method proposed in [28], and show that our method outperforms both, achieving higher directivity, narrower beamwidth and improved side-lobe suppression. We then compare the DoA estimation using the proposed method with MUSIC [9], ESPRIT [10], robust MVDR beamforming [21, 22], nested-array MVDR beamforming [23], and reduced dimension MVDR beamforming [24] methods, and show that our method works better even in low SNR scenarios. The proposed method is able to provide beamforming output, and can be used to estimate target directions, simultaneously.

The rest of the paper is organised as follows: Section II discusses the system model in the context of array signal processing using a uniform linear array (ULA). Section III explains the proposed feedback beamforming structure using an array. Section IV discusses the performance parameters, and Section V discusses the use of MVDR with feedback beamforming for DoA estimation. Section VI shows the comparison of beam-pattern and its performance parameters, and performance of DoA estimation method with prior methods. Finally, Section VII concludes the discussion.

II. SYSTEM MODEL

Consider the narrowband DoA estimation problem, where the reflected signal from L number of targets is captured using an N -element uniform linear array (ULA). At any time n , the received signal vector can be written as

$$\mathbf{r}[n] = \sum_{k=1}^L a_k[n] \mathbf{v}(\psi_k) + \mathbf{w}[n]. \quad (1)$$

Here, $\mathbf{v}(\psi_k) = [1 \ e^{-j\psi_k} \ \dots \ e^{-j(N-1)\psi_k}]$, $\psi_k = \frac{2\pi d}{\lambda} \cos \theta_k$ is the spatial frequency, λ is the operating wavelength, d is the inter-element spacing of ULA, and \mathbf{w} is complex additive white Gaussian noise with zero mean and variance σ^2 . The spatial frequency ψ_k depends on the angle of arrival θ_k of the returned signal, and is measured from the array axis. The targets are assumed to be stationary, and the reflected signals from each target are assumed to be uncorrelated with each other [29].

The model shown in (1) is closely related to the sum-of-complex-exponential model that has been used in several other problems, cf. [5–7, 10]. Therefore, the solution discussed here

can be generalised to different problems, when presented in this form.

We aim to estimate ψ_k from \mathbf{r} . As mentioned in Section I, several methods exist to solve such systems. In this work, we take the approach of estimating the parameters ψ_k using the MVDR [4] beamforming method, and incorporate it with spatial IIR feedback beamforming [28]. We compare the performance parameters of the beam-pattern, viz. beamwidth, first side-lobe level and directivity, with the feedback beamformer and conventional FIR beamformers that have been used in past work. We then use the MVDR IIR structure to estimate ψ_k , and show that our approach outperforms the existing methods in terms of requiring a lower SNR, and possessing a smaller beamwidth, thus resulting in finer resolution and higher side-lobe suppression.

III. FEEDBACK BEAMFORMING

There are multiple approaches for constructing spatial IIR beamformers. We enumerate them below.

- Case 1: No feedback (FIR)
- Case 2: Feedback without retransmission
- Case 3: Feedback with retransmission using a single antenna
- Case 4: Feedback with retransmission using an antenna array

Case 1 is the conventional beamformer, wherein the beamformer response can be modelled similar to that of a discrete-time FIR filter. Case 2 was introduced in [27], where the delay-like elements in the feedback depend on an initial estimate of ψ_k , and are iteratively refined over time using approaches such like recursive least-squares (RLS). Cases 3 and 4 involve retransmission based methods, which is the closest to a discrete-time IIR filter based approach. Case 3 was proposed in [28], where the captured signal is retransmitted using a single transmitting antenna. The approach in [28] is specific to the case of a single transmit antenna, and does not extend directly to the case of multiple antennas. The case of multiple antennas is, however, interesting from a practical point of view, since several recent radar applications involve situations where multiple antennas exist and can be exploited to enhance performance. Therefore, we present Case 4, which is the multi-antenna retransmission concept, wherein the retransmission is performed using an array, as opposed to a single element.

Overall, the goal is to design the beamformer weights based on an appropriate optimality criterion. One way to achieve this is to maximise the Fisher information of the beamformer output. Given (1) as the signal captured by the antenna array, the beamformer output is

$$y[n] = \boldsymbol{\beta}^H \mathbf{r}[n] \quad (2)$$

where $\boldsymbol{\beta} = [\beta_0 \ \dots \ \beta_{N-1}]^T$ is the beamformer weight vector. The Fisher information in the output is

$$J(\psi) = \Re \left\{ \frac{1}{2\pi\sigma^2} \int_{-\omega_s/2}^{\omega_s/2} \left| \frac{\partial Y(e^{j\omega})}{\partial \psi} \right|^2 d\omega \right\} \quad (3)$$

where $Y(e^{j\omega})$ is the discrete-time Fourier transform of $y[n]$, ω_s is the bandwidth of interest, σ^2 is noise spectral density, and $\Re\{\cdot\}$ denotes the real part. Maximising $J(\psi)$ with respect to β yields optimum beamformer weights. We will use this approach to obtain the beamformer weights of the proposed method as well.

A. Feedback with retransmission using single antenna

The feedback beamforming as explained in [28] is shown in Fig.1. The signal in the feedback path is retransmitted

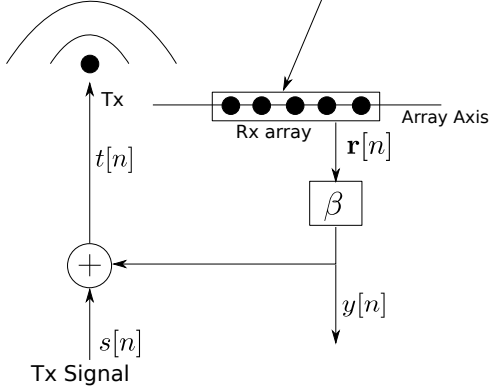


Fig. 1. Feedback beamforming block diagram with single transmitting antenna.

using only a single isotropic transmitting antenna. The diagram shown here is a simplified version of what is shown in [28], since the optimum feedback coefficients obtained by maximising the Fisher information matrix (FIM) is the same as the beamformer weights β . Therefore, combining both the paths result in the structure shown in Fig.1. The overall feedback beamformer response is given as:

$$H_{\text{single}}(\psi) = \frac{\beta^H \mathbf{v}(\psi)}{1 - \beta^H \mathbf{v}(\psi)} \quad (4)$$

where $\beta = [\beta_0 \dots \beta_{N-1}]^T$. The beamformer response in the case of a conventional FIR beamformer is $H_{\text{FIR}}(\psi) = \beta^H \mathbf{v}(\psi)$. From (4), it can be seen that because of the feedback, the beamformer response also has the denominator term when compared to $H_{\text{FIR}}(\psi)$. This is explained in detail in [28]. In the proposed work, we focus on obtaining the angle (θ) information only, and hence we discard the parameter ϕ used in [28] that is associated with range estimation, and omit the estimation of signal powers $P_k = \mathbb{E}(|a_k|^2)$.

B. Retransmitting feedback with Array

Extending the previous concept, we propose a retransmission method using an array instead of a single element. The modified block diagram is shown in Fig.2.

Unlike in the previous case, the transmit signal is directional, since we are using an array instead of a single isotropic element. The overall beamformer transfer function is given as:

$$H_{\text{array}}(\psi) = \frac{\beta^H \mathbf{v}(\psi)}{1 - \alpha^H \mathbf{v}(\psi) \beta^H \mathbf{v}(\psi)}. \quad (5)$$

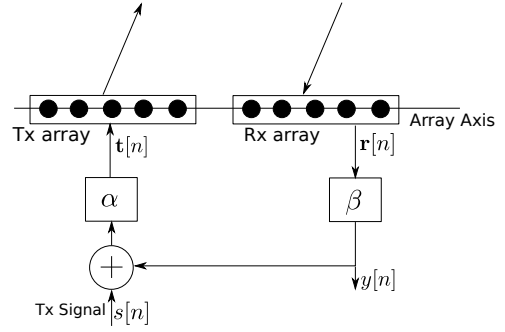


Fig. 2. Feedback beamforming block diagram with transmitting antenna array.

Comparing (5) with (4), the denominator possesses both α and β , which contributes to higher directivity. In the case where there is a single target at ψ , the optimal weights α and β are obtained by maximising the FIM:

$$\beta(\psi) = \frac{k\mathbf{v}(\psi)}{N}, \quad (6)$$

and $\alpha(\psi) = \frac{\mathbf{v}(\psi)}{kN}$, $k \in \mathbb{C} - \{0\}$.

Both (5) and (6) are derived in Appendix A.

IV. PERFORMANCE PARAMETERS

In this section, we derive the performance parameters of the proposed beamformer, viz. Half-Power beamwidth (HPBW), First Side-Lobe Level (FSL) and directivity using the generalised beam-pattern expression,

$$H_{\text{array}}(\psi) = \frac{g\beta^H \mathbf{v}(\psi)}{1 - g\beta^H \mathbf{v}(\psi) \alpha^H \mathbf{v}(\psi)} \quad (7)$$

where g is the received signal gain. In the following sections, we refer to $H_{\text{array}}(\cdot)$ as $H(\cdot)$ only. The beamformer weights α and β are dependent on the spatial frequency ψ as shown in (6). Assuming that the target spatial frequency is ψ_0 , the beam-pattern can be obtained as a function of ψ :

$$B(\psi) = |H(\psi)| = \left| \frac{\beta^H(\psi) \mathbf{v}(\psi_0)}{1 - \beta^H(\psi) \mathbf{v}(\psi_0) \alpha^H(\psi) \mathbf{v}(\psi_0)} \right|. \quad (8)$$

Using (6) in (8),

$$B(\psi) = \frac{\frac{\sin(N(\psi-\psi_0)/2)}{\sin((\psi-\psi_0)/2)}}{1 - \left(\frac{\sin(N(\psi-\psi_0)/2)}{\sin((\psi-\psi_0)/2)} \right)^2} \quad (9)$$

which is a standard beam-pattern expression. If the feedback filter α is removed, (8) reduces to the conventional FIR beamformer response $B_{\text{FIR}}(\psi) = |H_{\text{FIR}}(\psi)| = |\beta^H \mathbf{v}(\psi)|$.

A. Half-Power Beamwidth (HPBW)

Assuming the filter gain $\hat{g} \neq g$, we have

$$\beta(\psi) = \frac{\mathbf{v}(\psi)}{\hat{g}N} \quad \text{and} \quad \alpha(\psi) = \frac{\mathbf{v}(\psi)}{kN}. \quad (10)$$

Substituting values in (7), we obtain the maximum gain as

$$H(\psi) \Big|_{\max} = \frac{\frac{g}{\hat{g}}}{1 - \frac{g}{k\hat{g}}} = \frac{r}{1 - \frac{r}{k}} \quad (11)$$

where k is tunable to ensure that the denominator can always be made zero. Hence, ideally, the beamwidth remains zero regardless of the gain \hat{g} , compared to the HPBW of single element feedback [28] $\frac{1.4}{f(r)N}$, which is a function of the gain mismatch $r = \frac{g}{\hat{g}}$.

B. First Side-lobe Level

The side-lobe (secondary) peaks of $H(\psi)$ are at

$$\psi - \psi_0 = \frac{2m+1}{N}\pi, \quad \forall m \in \mathbb{Z} - \{0\}. \quad (12)$$

Hence the first side-lobe is at $m = 1$, which is $\Delta\psi = \frac{3\pi}{N}$. For a large enough N , from (9) we have

$$\begin{aligned} \text{FSL}(N) &= \left| r \frac{\frac{\sin 3\pi/2}{\sin 3\pi/2N}}{1 - \frac{r}{k} \left(\frac{\sin 3\pi/2}{\sin 3\pi/2N} \right)^2} \right|^2 \\ &\approx \frac{9\pi^2 k^2}{4N^2} \left(1 + \frac{9\pi^2}{2N^2} \right) \rightarrow \mathcal{O}(N^{-2}) \end{aligned} \quad (13)$$

which is independent of the gain mismatch r , and

$$\lim_{N \rightarrow \infty} \text{FSL}(N) \rightarrow 0. \quad (14)$$

C. Directivity

The maximum directivity D is defined as

$$D = \frac{H(\psi)|_{\max}}{\frac{1}{2\pi} \int_0^{2\pi} H(\psi) d\psi} = \frac{\frac{2\pi r}{1 - \frac{r}{k}}}{\int_0^{2\pi} H(\psi) d\psi}. \quad (15)$$

In this case, $H(\psi)|_{\max}$ is tunable, hence directivity is a function of the tuning parameter k .

V. ARRAY FEEDBACK BEAMFORMING FOR DOA ESTIMATION USING MVDR

We now present the proposed approach to estimate the ψ parameters using MVDR with feedback beamforming for the model shown in (1). Fig.3 shows the block diagram depicting how MVDR can be used with a feedback beamforming structure.

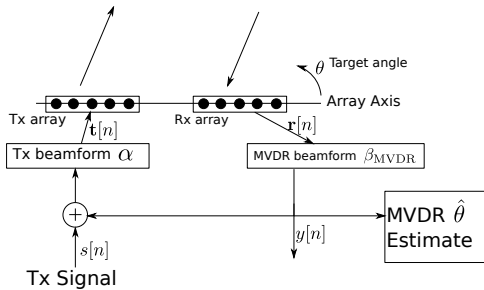


Fig. 3. Block diagram of MVDR DoA estimation using feedback beamforming.

As shown in Fig.3, the signal is first captured using a ULA, and the received signal \mathbf{r} as in (1) is used to compute the MVDR coefficients. Given the autocorrelation matrix $\mathbf{R}_{\mathbf{r}\mathbf{r}} =$

$\frac{1}{N_{\text{samples}}} \sum_{n=1}^{N_{\text{samples}}} \mathbf{r}[n] \mathbf{r}^H[n]$ and a linear constraint $\boldsymbol{\beta}^H \mathbf{c} = 1$, the MVDR coefficients can be computed as:

$$\boldsymbol{\beta}_{\text{MVDR}} = \frac{\mathbf{R}_{\mathbf{r}\mathbf{r}}^{-1} \mathbf{c}}{\mathbf{c}^H \mathbf{R}_{\mathbf{r}\mathbf{r}}^{-1} \mathbf{c}} \quad (16)$$

where N_{samples} are the available number of time-samples.

Next, the feedback (retransmission) coefficients α are inferred from β , and over multiple such retransmissions, the coefficients get stabilised. At this point, ψ parameters are estimated using α and β . Depending on the approach taken to infer α from β , there are two possible methods to estimate α , as shown in Algorithm 1 and Algorithm 2.

The classical MVDR method was primarily designed to mitigate/suppress interference, but here we utilise the same functionality to find the target directions instead. Typically, the MVDR weights are computed in the absence of the targets and in the presence of interference and jammers, so that the algorithm steers the beamformer nulls in the directions where the interferers and jammers are present while maintaining distortionless response in a desired direction. However, in the presence of targets, the MVDR method computes the beamformer weights such that nulls are placed along the target directions. The constraint vector in (16) is taken as $\mathbf{c} = [1 \dots e^{-j(N-1)\psi}]^T$ that allows an undistorted response from the desired direction. This constraint is used for Algorithm 1.

Algorithm 1

- 1: Start with β as in (16).
- 2: Formulate $\alpha = \mathbf{c} = [1 \ e^{-j\psi} \ \dots \ e^{-j(N-1)\psi}]^T$
- 3: Sweep ψ in the visible region (typically $[-\pi, \pi)$). If a target angle coincides with the sweep angle, the response at that angle peaks while suppressing contribution of all the other targets.
- 4: Transmit vector = $\alpha(\psi)$

The same constraint vector \mathbf{c} can be changed to any other linear constraint vector, as long as the algorithm produces computable beamformer weights. A simple choice is $\mathbf{c} = [1 \ 0 \ \dots \ 0]^T$, that ensures the first element of β , that is β_0 , is always 1. This constraint is used for Algorithm 2.

Algorithm 2

- 1: Start with β as in (16) using $\mathbf{c} = [1 \ \dots \ 0]^T$. The nulls of β appear along the target directions.
- 2: Formulate α as impulse response of $1/\beta(\psi)$
- 3: The nulls in $\beta(\psi)$ result as peaks in $\alpha(\psi)$
- 4: Transmit vector = $\alpha(\psi)$

Both methods yield iteratively better estimates, even if the initial estimates are inaccurate. We discuss and compare the performance of both methods in the next section.

VI. RESULTS AND DISCUSSION

In this section, via simulations, we first show the beam-pattern and FSL, as discussed in Section IV for the proposed beamforming method. We then show the performance of the

DoA estimation using the proposed method and compare it with previous methods, viz. MUSIC [9], ESPRIT [10], Robust Capon beamforming [21, 22], nested array beamforming [23], and reduced dimension beamforming [24].

A. Beam-pattern and performance parameters

We consider a 3-element ULA, with inter-element spacing $\lambda/2$, and assume a target present at $\theta = \pi/3$. We plot the beamformer response for all angles $\theta \in [0, \pi)$ and compare the beam-pattern parameters of the proposed method with that of existing methods.

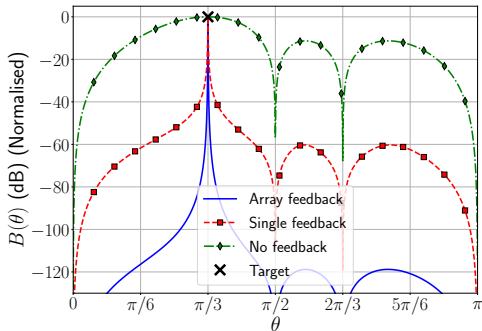


Fig. 4. Comparing beam-pattern of array feedback beamformer with single feedback and conventional FIR beamformers

In Fig. 4, we compare the beam-pattern of the proposed feedback beamforming with existing feedback beamforming methods [28] and the conventional FIR method. The HPBW of the FIR beamformer is limited by the number of elements, and that of the feedback beamformer is a function of gain mismatch. Compared to the single element feedback case, the HPBW of the proposed approach is 50% less, which is consistent with the reduction predicted in theory. The side-lobe level of the feedback beamformer is 50 dB below conventional FIR beamformer, while that for the proposed method, it is even lower, at 110 dB. The proposed method outperforms both the conventional FIR beamformer and feedback beamformer [28] in terms of side-lobe suppression and beamwidth.

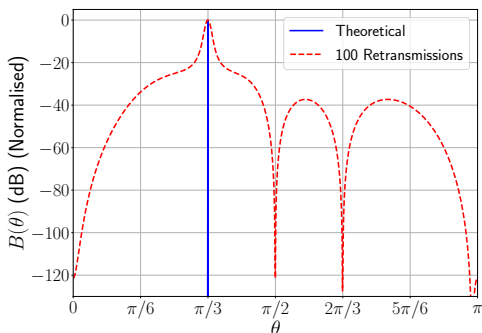


Fig. 5. Beam-pattern after finite (100) retransmission time-stamps

Fig. 5 shows the comparison of an ideal feedback beamformer with that of a realisable one. In practice, the IIR-like performance can be achieved only approximately, because of the finite number of snapshots that are available. Even then,

the proposed method achieves an HPBW that is 90% lower than that obtained using FIR beamformers.

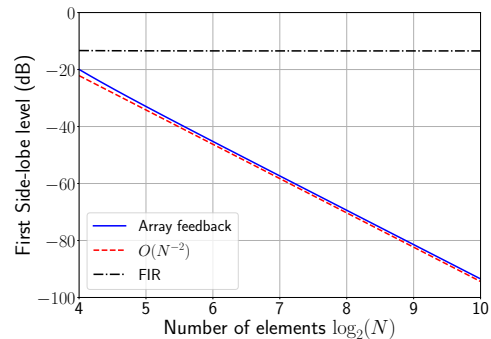


Fig. 6. First Side-lobe level trend with number of array elements.

Fig. 6 shows the absolute value of FSL for different numbers of array elements. According to (13), the FSL decreases as $\mathcal{O}(N^{-2})$, and is independent of the gain mismatch r , as opposed to the FIR beamformer, where the FSL remains constant at ~ -13.5 dB. Even with as few as 16 elements, the level difference is 7 dB, and it decreases fast with increasing number of elements. At 1024 elements, the difference is around 100 dB.

B. Direction Estimation

As discussed in Section V, we can use the MVDR with feedback beamforming to estimate ψ from \mathbf{r} in (1). We use Algorithm 1 and Algorithm 2 shown in Section V and compare the resultant estimation error with MUSIC and ESPRIT for various SNR levels. We also consider inter-element spacing in the ULA $d = \lambda/2$, hence $\psi = \pi \cos \theta$. We take an 8-element ULA, and assume 4 targets at distinct angles $\theta_1, \theta_2, \theta_3, \theta_4$. The signals reflected from these targets are considered uncorrelated with each other. The received signal at the array is assumed to follow the model in (1).

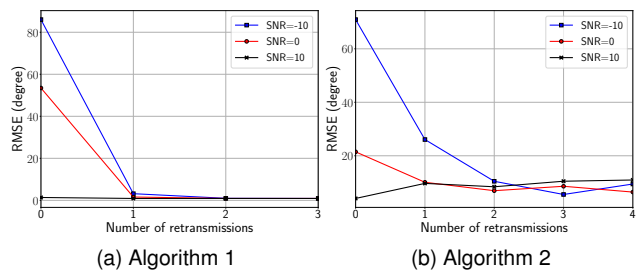


Fig. 7. RMS error of MVDR DoA estimation using feedback beamforming with respect to number of retransmissions for SNR -10, 0, and 10 dB

Fig. 7 shows the root-mean-squared error (RMSE) for three different levels of SNR. Since our goal is to target the low SNR region, we consider SNR = -10 dB, 0 dB, and 10 dB. Fig. 7b and Fig. 7a show the performance for Algorithm 1 and Algorithm 2 discussed in Section V, respectively. From Fig. 7 it can be seen that, for no retransmission, the estimation error is large, since feedback is absent. As the number of retransmissions increases, the error reduces rapidly for both

methods. Comparing Fig. 7b and Fig. 7a, it is evident that Algorithm 1 yields better estimates than Algorithm 2, since the error reduces faster for Algorithm 1.

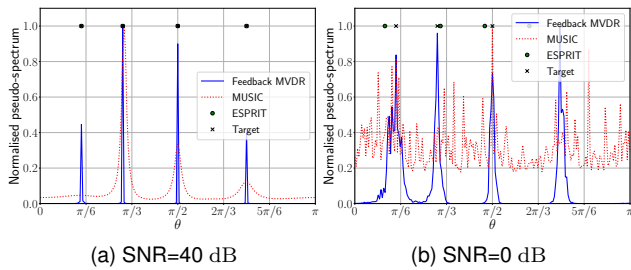


Fig. 8. Comparison of feedback MVDR with 2 retransmissions with MUSIC and ESPRIT

Fig.8 shows the angle estimation performance compared to MUSIC and ESPRIT. For this, we use Algorithm 1. The array steering direction θ is varied from 0 to π , and the transmit weight vector α varies accordingly with the constraint \mathbf{c} . The beamformer response is computed as y_ψ , and the pseudo-spectrum is computed as $P_{\text{out}}(\psi) = \frac{1}{N_{\text{samples}}} \sum_n y_\psi[n] y_\psi^*[n]$, $\forall \psi$. Fig.8 shows the normalised pseudo-spectrum as a function of θ .

It can be seen that, with as low as just two retransmissions, the feedback beamformer is able to achieve angle estimates at par with that of ESPRIT at high SNR. However, for both MUSIC and ESPRIT, the number of targets L is known, which is not a constraint for the proposed feedback MVDR method. Even at 0 dB SNR, the proposed method shows better estimates than both MUSIC and ESPRIT.

Finally, in Fig.9 we compare the DoA estimation error of the proposed method with previous methods for different SNR values in the following manner. We consider $N = 8$ -element ULA with $d = \lambda/2$ inter-element spacing. We assume two targets at θ_1 and θ_2 , and the return signal is modelled as in (1). For MUSIC [9] and ESPRIT [10], we consider this ULA and find the estimates $\hat{\theta}_1$ and $\hat{\theta}_2$. For robust MVDR [21, 22], we assume the regularising parameter $\lambda_r = 0.05$, which is suitably chosen within the bounds [22], and then $\hat{\theta}_1$ and $\hat{\theta}_2$ are estimated. For Nested array [23] setup, we consider level-1 subarray of $N_1 = \lfloor N/2 \rfloor = 4$ elements with inter-element spacing $d_1 = d = \lambda/2$ and level-2 subarray of $N_2 = \lceil N/2 \rceil = 4$ elements with inter-element spacing $d_2 = (N_1 + 1)d = 5\lambda/2$, and then perform the necessary rearrangement of the elements of the autocorrelation matrix \mathbf{R}_{rr} to estimate $\hat{\theta}_1$ and $\hat{\theta}_2$. For reduced dimension MVDR [24], we consider 4 subarrays of $L = 2$ elements each from the ULA, and use Algorithm 1 (SAMVDR) from [24] to estimate $\hat{\theta}_1$ and $\hat{\theta}_2$. We then find the root-mean-squared error as $\sqrt{\sum_{k=1}^2 (\theta_k - \hat{\theta}_k)^2}$ and take an average over 100 Monte-Carlo runs.

From Fig.9 it is evident that feedback MVDR yields better error performance than all considered methods. Robust MVDR yields better estimation error after 0 dB SNR, while all other methods perform better only after 40 dB SNR. While these methods primarily work better at higher SNR levels, our method works even at the low SNR range of -60 dB to

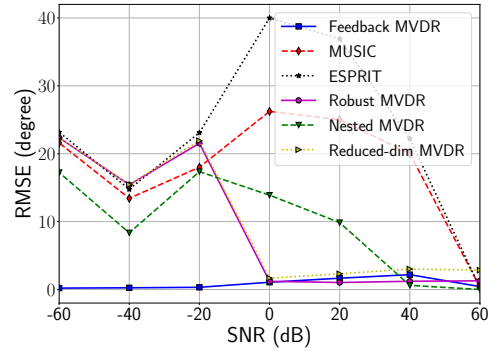


Fig. 9. Comparison of RMSE with respect to SNR of feedback MVDR with prior methods.

-10 dB. The RMSE of the proposed method is 20° less than all methods in the low SNR region.

VII. CONCLUSION

We propose a novel approach to the problem of spatial filtering, beamforming and DoA estimation using the feedback beamforming method with a retransmitting array. We apply this approach to a ULA to derive the beam-pattern performance parameters. Through extensive simulations, we show that our method outperforms the conventional FIR beamformer and previously presented IIR beamforming structures in terms of better side-lobe suppression, higher directivity, and narrower beamwidth. Then, we propose a method to incorporate MVDR into this feedback structure and show that the combined architecture is able to provide beamforming output, and can be used to estimate the target directions. The proposed method outperforms conventional DoA estimation methods MUSIC and ESPRIT, and other MVDR variants, in terms of achieving better accuracy and better target separation. The proposed method is arguably better in the low-SNR regime, and yields 20° lower estimation error, and hence is useful for applications with stringent SNR constraints.

APPENDIX

Here we will derive the beamformer weights α and β by maximising the Fisher information matrix. Consider the signal $s[n]$ that is transmitted using the N_t -element transmitting array, along with the feedback component. The transmitted signal from the k th element of the array at time n is given as

$$t_k[n] = \delta_k s[n] + \alpha_k^* y[n - \tau_k], \quad \delta_k = \begin{cases} 1 & : k = 0 \\ 0 & : \text{otherwise} \end{cases}$$

where $k = 0, \dots, N_t - 1$, and $(\cdot)^*$ denotes complex conjugate. Similarly, the signal received from a single target located at ψ at the l th element of the N_r -element receiving array is given as

$$\begin{aligned} r_l[n] &= \sum_k t_k[n - \tau_l - \tau_R] \\ &= s[n - \tau_l - \tau_R] + \sum_k \alpha_k^* y[n - \tau_k - \tau_l - \tau_R] \end{aligned}$$

where $k = 0, \dots, N_t - 1$ and $l = 0, \dots, N_r - 1$. τ_l and τ_k are the delays due to the array geometry, and τ_R is the delay due to the target range. Converting r_l to frequency domain,

$$R_l(e^{j\omega}) = \left(S(e^{j\omega}) + \sum_k \alpha_k^* e^{-j\omega\tau_k} Y(e^{j\omega}) \right) e^{-j\omega(\tau_l + \tau_R)}$$

where $R_l(e^{j\omega})$, $S(e^{j\omega})$, and $Y(e^{j\omega})$ are the discrete-time Fourier transforms of $r_l[n]$, $s[n]$ and $y[n]$, respectively.

The beamformer output is given as

$$\begin{aligned} Y(e^{j\omega}) &= \sum_l \beta_l^* R_l(e^{j\omega}) \\ &= \left(S(e^{j\omega}) + \sum_k \alpha_k^* e^{-j\omega\tau_k} Y(e^{j\omega}) \right) \sum_l \beta_l^* e^{-j\omega\tau_l} e^{-j\omega\tau_R}. \end{aligned}$$

Hence, the transfer function at ω is given as

$$H(e^{j\omega}) = \frac{Y(e^{j\omega})}{S(e^{j\omega})} = \frac{\sum_l \beta_l^* e^{-j\omega\tau_l} e^{-j\omega\tau_R}}{1 - \sum_l \beta_l^* e^{-j\omega\tau_l} \sum_k \alpha_k^* e^{-j\omega\tau_k} e^{-j\omega\tau_R}}.$$

Considering the narrowband signal model, for ULA, $\tau_l = l\tau$ and $\tau_k = k\tau$ for $k, l = 0, 1, \dots, N - 1$ assuming $N_t = N_r = N$. Taking $\omega\tau = \frac{2\pi}{\lambda} d \cos \theta = \psi$, and single frequency ω_0

$$H(\psi, \phi) = \frac{\beta^H \mathbf{v}(\psi) e^{-j\phi}}{1 - \beta^H \mathbf{v}(\psi) \alpha^H \mathbf{v}(\psi) e^{-j\phi}}$$

where $\mathbf{v}(\psi) = [1 \ e^{-j\psi} \ e^{-2j\psi} \ \dots \ e^{-j(N-1)\psi}]^T$ and $\phi = \omega\tau_R$. This expression is shown in (5).

We formulate the Fisher Information Matrix as below:

$$\mathbf{J} = \begin{bmatrix} J_{\psi\psi} & J_{\psi\phi} \\ J_{\phi\psi} & J_{\phi\phi} \end{bmatrix}$$

where $J_{\psi\phi} = J_{\phi\psi}^*$. Each term J_{pq} can be computed as

$$J_{pq} = \Re \left\{ \frac{1}{2\pi\sigma^2} \int_{-\frac{\omega_s}{2}}^{\frac{\omega_s}{2}} \left(\frac{\partial Y(e^{j\omega})}{\partial p} \right)^* \left(\frac{\partial Y(e^{j\omega})}{\partial q} \right) d\omega \right\}$$

where $\Re\{\cdot\}$ denotes real part, $p, q \in \{\psi, \phi\}$, ω_s is the bandwidth, and σ^2 is the noise spectral density. Hence,

$$\begin{aligned} \frac{\partial Y(e^{j\omega})}{\partial \psi} &= \frac{\beta^H (\mathbf{I} + \mathbf{v}(\psi) \beta^H \mathbf{v}(\psi) \alpha^H e^{-j\phi}) \mathbf{A} \mathbf{v}(\psi) e^{-j\phi}}{(1 - \beta^H \mathbf{v}(\psi) \alpha^H \mathbf{v}(\psi) e^{-j\phi})^2} S(e^{j\omega}) \\ \frac{\partial Y(e^{j\omega})}{\partial \phi} &= \frac{-j \beta^H \mathbf{v}(\psi) e^{-j\phi}}{(1 - \beta^H \mathbf{v}(\psi) \alpha^H \mathbf{v}(\psi) e^{-j\phi})^2} S(e^{j\omega}) \end{aligned}$$

All the terms of \mathbf{J} can be computed as:

$$J_{\psi\psi} = \frac{1}{2\pi\sigma^2} \int_{-\frac{\omega_s}{2}}^{\frac{\omega_s}{2}} \left| \frac{\beta^H (\mathbf{I} + \mathbf{v}(\psi) \beta^H \mathbf{v}(\psi) \alpha^H e^{-j\phi}) \mathbf{A} \mathbf{v}(\psi)}{(1 - \beta^H \mathbf{v}(\psi) \alpha^H \mathbf{v}(\psi) e^{-j\phi})^2} \right|^2 |S(e^{j\omega})|^2 d\omega$$

$$J_{\phi\phi} = \frac{1}{2\pi\sigma^2} \int_{-\frac{\omega_s}{2}}^{\frac{\omega_s}{2}} \left| \frac{\beta^H \mathbf{v}(\psi)}{(1 - \beta^H \mathbf{v}(\psi) \alpha^H \mathbf{v}(\psi) e^{-j\phi})^2} \right|^2 |S(e^{j\omega})|^2 d\omega$$

$$J_{\psi\phi} = \Re \left\{ \frac{j}{2\pi\sigma^2} \int_{-\frac{\omega_s}{2}}^{\frac{\omega_s}{2}} \frac{\beta^H (\mathbf{I} + \mathbf{v}(\psi) \beta^H \mathbf{v}(\psi) \alpha^H e^{-j\phi}) \mathbf{A} \mathbf{v}(\psi) \mathbf{v}(\psi)^H \beta}{(1 - \beta^H \mathbf{v}(\psi) \alpha^H \mathbf{v}(\psi) e^{-j\phi})^4} \right\} |S(e^{j\omega})|^2 d\omega$$

where $\mathbf{A} = \text{diag}([0 \ -j \ -2j \ \dots \ -j(N-1)])$. Maximising this FIM results in the weights to be

$$\begin{aligned} \beta &= \frac{k\mathbf{v}(\psi)}{N} e^{-j(1-l)\phi}, \text{ and} \\ \alpha &= \frac{\mathbf{v}(\psi)}{kN} e^{-jl\phi}, \quad k \in \mathbb{C} - \{0\}, \quad l \in [0, 1]. \end{aligned}$$

This expression is shown in (6) in Section III without the parameter ϕ .

REFERENCES

- [1] Simon Haykin, "Cognitive radar: a way of the future," *IEEE signal processing magazine*, vol. 23, no. 1, pp. 30–40, 2006.
- [2] Yongzhe Li, Sergiy A Vorobyov, and Aboulnahr Hassanien, "Robust Beamforming for Jammers Suppression in MIMO Radar," in *2014 IEEE Radar Conference*. IEEE, 2014, pp. 0629–0634.
- [3] Fan Liu, Christos Masouros, Ang Li, and Tharmalingam Ratnarajah, "Robust MIMO Beamforming for Cellular and Radar Coexistence," *IEEE Wireless Commun. Lett.*, vol. 6, no. 3, pp. 374–377, 2017.
- [4] Harry L Van Trees, *Optimum Array Processing: Part IV of Detection, Estimation, and Modulation Theory*, John Wiley & Sons, 2002.
- [5] Martin Vetterli, Pina Marziliano, and Thierry Blu, "Sampling Signals with Finite Rate of Innovation," *IEEE Trans. Signal Process.*, vol. 50, no. 6, pp. 1417–1428, 2002.
- [6] Tapan K Sarkar and Odilon Pereira, "Using the Matrix Pencil Method to Estimate the Parameters of a Sum of Complex Exponentials," *IEEE Antennas Propag. Mag.*, vol. 37, no. 1, pp. 48–55, 1995.
- [7] Prajakta Sathe and Amitabha Bhattacharya, "Automatic Object Discrimination Based on Natural Resonant Features of Dielectric Coated Objects," *IEEE Trans. Antennas Propag.*, 2022.
- [8] Arun Venkitaraman and Pascal Frossard, "Annihilation Filter Approach for Estimating Graph Dynamics from Diffusion Processes," in *ICASSP 2022-2022 IEEE International Conference on Acoustics, Speech and Signal Processing (ICASSP)*. IEEE, 2022, pp. 5583–5587.
- [9] R. Schmidt, "Multiple Emitter Location and Signal Parameter Estimation," *IEEE Trans. Antennas Propag.*, vol. 34, no. 3, pp. 276–280, 1986.
- [10] Richard Roy and Thomas Kailath, "ESPRIT-Estimation of Signal Parameters via Rotational Invariance Techniques," *IEEE Trans. Acoust., Speech, Signal Process.*, vol. 37, no. 7, pp. 984–995, 1989.
- [11] ZI Khan, M MD Kamal, N Hamzah, K Othman, and NI Khan, "Analysis of Performance for Multiple Signal Classification (MUSIC) in Estimating Direction of Arrival," in *2008 IEEE International RF and Microwave Conference*. IEEE, 2008, pp. 524–529.
- [12] Ahmet M Elbir, "DeepMUSIC: Multiple Signal Classification via Deep Learning," *IEEE Sensors Letters*, vol. 4, no. 4, pp. 1–4, 2020.
- [13] HK Hwang, Zekeriya Aliyazicioglu, Marshall Grice, and Anatoly Yakovlev, "Direction of Arrival Estimation using a Root-MUSIC Algorithm," in *Proceedings of the International MultiConference of Engineers and Computer Scientists*. Citeseer, 2008, vol. 2, pp. 19–21.
- [14] Feifei Gao and Alex B Gershman, "A Generalized ESPRIT Approach to Direction-of-Arrival Estimation," *IEEE Signal Process. Lett.*, vol. 12, no. 3, pp. 254–257, 2005.
- [15] Jens Steinwandt, Florian Roemer, and Martin Haardt, "Generalized Least Squares for ESPRIT-Type Direction of Arrival Estimation," *IEEE Signal Process. Lett.*, vol. 24, no. 11, pp. 1681–1685, 2017.
- [16] Huiping Duan, Boon Poh Ng, and Chong Meng See, "A New Broadband Beamformer Using IIR Filters," *IEEE Signal Process. Lett.*, vol. 12, no. 11, pp. 776–779, 2005.
- [17] Shefeng Yan, "Optimal Design of FIR Beamformer With Frequency Invariant Patterns," *Applied Acoustics*, vol. 67, no. 6, pp. 511–528, 2006.
- [18] Huiping Duan, Boon Poh Ng, Chong Meng Samson See, and Jun Fang, "Broadband Beamforming using TDL-Form IIR Filters," *IEEE Trans. Signal Process.*, vol. 55, no. 3, pp. 990–1002, 2007.
- [19] Daniele Salvati, Carlo Drioli, and Gian Luca Foresti, "On the use of Machine Learning in Microphone Array Beamforming for Far-Field Sound Source Localization," in *2016 IEEE 26th International Workshop on Machine Learning for Signal Processing (MLSP)*. IEEE, 2016, pp. 1–6.
- [20] Ahmed Alkhateeb, Sam Alex, Paul Varkey, Ying Li, Qi Qu, and Djordje Tujkovic, "Deep Learning Coordinated Beamforming for Highly-Mobile Millimeter Wave Systems," *IEEE Access*, vol. 6, pp. 37328–37348, 2018.
- [21] Petre Stoica, Zhisong Wang, and Jian Li, "Robust Capon Beamforming," in *Conference Record of the Thirty-Sixth Asilomar Conference on Signals, Systems and Computers, 2002*. IEEE, 2002, vol. 1, pp. 876–880.
- [22] Jian Li, Petre Stoica, and Zhisong Wang, "On Robust Capon Beamforming and Diagonal Loading," *IEEE transactions on signal processing*, vol. 51, no. 7, pp. 1702–1715, 2003.
- [23] Zhi Zheng, Tong Yang, Di Jiang, and Wen-Qin Wang, "Robust and Efficient Adaptive Beamforming using Nested Subarray Principles," *IEEE Access*, vol. 8, pp. 4076–4085, 2019.
- [24] Tuanning Liu, Wenqiang Liu, Yuanping Zhou, and Kesong Fan, "Reduced-Dimension MVDR Beamformer Based on Sub-array Optimization," *IET Communications*, vol. 16, no. 18, pp. 2183–2192, 2022.
- [25] Alan V Oppenheim, John R Buck, and Ronald W Schaffer, *Discrete-*

- Time Signal Processing. Vol. 2*, Upper Saddle River, NJ: Prentice Hall, 2001.
- [26] A Antonion, “Digital Filters: Analysis, Design and Application,” *McGraw Hill, New York*, vol. 5, pp. 886896, 1993.
- [27] Fuxi Wen, Boon Poh Ng, and Vinod Veera Reddy, “Extending the Concept of IIR Filtering to Array Processing using Approximate Spatial IIR Structure,” *Multidimensional Systems and Signal Processing*, vol. 24, no. 1, pp. 157–179, 2013.
- [28] Itay Yehezkel Karo, Tsvi G Dvorkind, and Israel Cohen, “Source Localization with Feedback Beamforming,” *IEEE Trans. Signal Process.*, vol. 69, pp. 631–640, 2020.
- [29] GS Sandhu and AV Saylor, “A Real-Time Statistical Radar Target Model,” *IEEE Transactions on Aerospace and Electronic Systems*, , no. 4, pp. 490–507, 1985.